ELSEVIER

Catalysis Today 38 (1997) 339–360

CATALYSIS TODAY

Bifunctional pathways in catalysis by solid acids and bases[1]

Enrique Iglesia[a,*], David G. Barton[a], Joseph A. Biscardi[a], Marcelo J.L. Gines[a], Stuart L. Soled[b]

[a] *Department of Chemical Engineering, University of California at Berkeley and Materials Sciences Division, E.O. Lawrence Berkeley National Laboratory, Berkeley, CA 94720, USA*

[b] *Corporate Research Laboratory, Exxon Research and Engineering Co., Route 22 East, Annandale, NJ 08801, USA*

Abstract

Chemical reactions catalyzed by solid acids and bases often require that reactants, intermediates, or activated complexes interact with several surface functions. Concerted and sequential bifunctional pathways also occur in homogeneous and enzyme catalysis. Hydrogenation and dehydration reactions require acid–base site pairs of intermediate strength, because such sites can form, stabilize, and discard adsorbed intermediates during a catalytic turnover. Deuterium exchange and H–H dissociation reactions also occur on acid–base pairs present in single-component or binary oxides and in supported oxide clusters. Hydrogenation of aromatic acids, dehydration of alkanols and methanolamine, condensation of alcohols, and deuterium exchange provide specific examples of bifunctional acid–base catalysis. Dehydration and dehydrogenation reactions of alkanols, widely used as probes of acid or base sites, probe instead the density and chemical properties of acid–base site pairs. Concerted bifunctional pathways require that sites co-exist within molecular distances. On surfaces, the inappropriate location of these sites can prevent concerted interactions, but rapid transfer of intermediates via surface or gas phase diffusion leads to kinetic coupling between distant sites and to sequential bifunctional pathways. These bifunctional sequences overcome proximity requirements by equilibration of adsorbed species throughout surface regions containing several types of sites. Diffusion of alkenes in the gas phase couples dehydrogenation and acid sites during *n*-alkane isomerization on bifunctional tungsten carbides modified by chemisorbed oxygen. These bifunctional surfaces form Bronsted acid sites by surface migration of H adatoms from WC to WO_x sites. Acid (or base) sites and H_2 dissociation sites on surfaces interact via surface diffusion of H adatoms. This leads to bifunctional alkane and alkanol reactions via kinetic coupling of C–H or O–H bond activation and hydrogen adsorption–desorption steps. Propane dehydrogenation on H-ZSM5 modified by exchanged cations, *n*-heptane isomerization on ZrO_2 doped with WO_x and Pt, and alcohol condensation on Cu-promoted Mg_5CeO_x oxides illustrate the role of kinetic coupling mediated by migration of hydrogen adatoms. In each example, metal clusters or isolated cations increase the rate of acid or base catalysis by providing a 'porthole' for hydrogen adsorption and desorption.

Keywords: Bifunctional pathway, concerted; Solid acid; Adatom migration

1. Introduction

The cooperative behavior of surface sites with acidic, basic, or reduction–oxidation properties is an essential requirement for catalysis on many inorganic

*Corresponding author. Tel.: (1-510) 642-9673; Fax: (1-510) 642-4778; e-mail: iglesia@cchem.berkeley.edu

[1]Based on a Plenary Address delivered at the International Symposium on Acid–Base Catalysis III, Rolduc, The Netherlands, April 20–24, 1997.

PII S0920-5861(97)00079-5

solids. This behavior finds analogs in homogeneous and enzymatic catalysis, in which solvent effects and amphoteric acid–base properties also lead to concerted and sequential interactions of reactants with acidic and basic sites. On the surfaces of inorganic solids, concerted interactions may be hindered by the fixed and inappropriate location of the required catalytic functions. In such cases, sequential interactions can still influence catalytic paths via migration of gas phase and surface intermediates. One specific example is the rapid migration of hydrogen species on surfaces at typical catalytic temperatures, which allows communication between acidic (or basic) sites and H_2 dissociation sites, leading to bifunctional activation of C–H bonds in alkanes and alkanols.

This review describes recent examples of bifunctional pathways in heterogeneous catalysis with emphasis on reactions requiring acidic or basic sites for one or more of the required catalytic steps. The chosen examples cover a wide range of catalytic reactions and materials in order to illustrate the ubiquitous requirement for multiple interactions between molecules and surfaces in the formation and conversion of reaction intermediates. The term bifunctional catalysis is used with some concern, because in some examples of acid–base catalysis the two required functions may consist simply of a conjugate acid–base pair.

2. Bifunctional pathways in homogeneous and enzymatic catalysis

An often cited example of bifunctional homogeneous catalysis is the mutarotation of glucose, which occurs much more rapidly in the presence of molecules containing weakly acidic and basic functions than on stronger basic or acidic molecules [1–4]. The concerted interaction of the OH group in tetramethylglucose with a basic group, such as the nitrogen atom in 2-hydroxy-pyridine, and the ring oxygen atom in glucose with the acidic OH group in 2-hydroxy-pyridine leads to reversible ring opening with intervening rotation along a C–C bond. Mutarotation reaction rates are much faster with 2-hydroxy-pyridine than with stronger acid catalysts, such as phenol, or stronger bases, such as pyridine, which lack a strong corresponding conjugate function. The presence of proton acceptor and donor species in 2-hydroxy-pyridine catalyzes the transfer of hydrogen from the OH to the ring oxygen in glucose with the concomitant opening of the glucose ring. Similarly, weak carboxylic acids catalyze these reactions much more efficiently than stronger mineral acids, because of the basic properties of the carbonyl oxygen in carboxylic acids [3,4].

The enzyme-catalyzed hydrolysis of phosphate diester linkages in RNA by ribonuclease A also appears to involve a concerted interaction of RNA with acidic and basic sites in the enzyme [5,6]. Hydrolysis rates of polyuridylic acid molecules, containing phosphate diester linkages similar to those in RNA, reach a maximum value when imidazole (Im) groups in enzyme mimics reach an intermediate state of protonation by varying the solution pH. Nitrogen groups in unprotonated imidazole abstract a proton from OH groups near ester linkages and the protonated imidazole (ImH^+) protonates one of the oxygen atoms in the phosphate group (Scheme 1) in a first step, followed by the addition of water to the terminal phosphate group. With homogeneous enzyme mimics, the acid and base catalytic species act in a sequential fashion. In actual enzymes, it is likely that the interactions of RNA with both functions occur in a concerted manner aided by the precise and fixed location of these functions within the enzyme molecule.

This concept of bifunctional acid–base pairs has also been used in the design of enzyme mimics for the cleavage of ester linkages in the deacylation of *p*-nitrophenyl acetate [6]. The synthesis of molecular

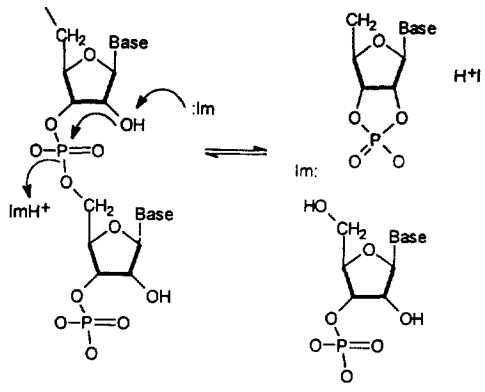

Scheme 1. Cleavage of phosphate diester linkages in ribonucleic acid via acid–base bifunctional catalysis [5].

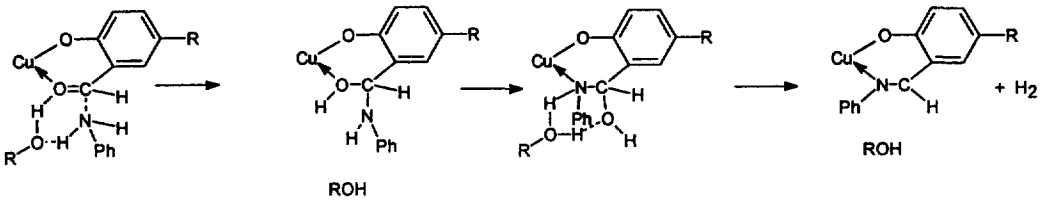

Scheme 2. Bifunctional acid–base pathways for the addition of aniline to coordinated salicylic aldehyde using alcohols (ROH) as co-catalysts [8].

catalysts containing a basic function provided by the nitrogen in a imidazolyl group and an acid function provided by an acidic OH group in a resorcinol moiety leads to much faster rates than on the individual basic and acid components or on mixtures of basic imidazole and acidic resorcinol molecules.

Bifunctional acid–base pathways are also involved in reactions catalyzed by cationic transition metal complexes. Halpern [7] showed that H_2 dissociation by Cu^{2+} ions in solution proceeds via a concerted interaction of the H_2 molecules with a Lewis acid (Cu^{2+}) and a basic oxygen in coordinated water molecules. H atoms associated with Cu centers retain a net negative charge, while H atoms interacting with water molecules acquire a net positive charge. Zamaraev et al. [8] have shown that the addition of aniline to derivatives of salicylic aldehydes using Cu^{2+} and Zn^{2+} as coordinating agents for the aldehydes proceeds via a hydrogen atom transfer involving acid–base pairs and requiring the presence of organic alcohol co-catalysts (Scheme 2). The organic alcohol co-catalyst acts as a Bronsted acid and the nitrogen group in aniline as the base in hydrogen transfer steps required for both the addition of aniline and the subsequent dehydration of the carbinolamine intermediate. The metal center acts as a coordinating agent, but appears to play a minor role in this concerted acid–base hydrogen transfer mechanism.

3. Early examples of bifunctional heterogeneous catalysis

Bifunctional reaction pathways in heterogeneous catalysis were first proposed for the isomerization of *n*-alkanes and naphthenes in catalytic reforming reactions [9,10]. Metal or redox sites catalyze dehydrogenation reactions and the resulting unsaturated intermediates are protonated on Bronsted acid sites. These protonated species then rearrange via carbocationic pathways similar to those proposed for the formation of isoalkenes and cyclic hydrocarbons using homogeneous liquid acids as catalysts. Isoalkenes are then hydrogenated on metal sites to form thermodynamically favored alkanes. This type of bifunctional catalysis involves the gas phase migration of unsaturated molecules between acid and metal sites over significant distances within catalyst pellets. Bifunctional dehydrogenation reactions were also proposed in order to explain the synergy between acid sites and Mo or Cr cations in the conversion of cyclohexane to benzene on Cr_2O_3/Al_2O_3 and MoO_x/Al_2O_3 catalysts [11]. Gas-phase intermediates are not likely to be involved in this type of synergistic behavior. The two sites are likely to communicate instead via the migration of hydrogen species from acid sites, where C–H bond cleavage may occur, to metal cation sites where H-adatoms are removed by recombinative desorption. A similar mechanism was proposed by Fujimoto et al. for dehydrogenation of *n*-alkanes on carbon-supported Pt catalysts [12]. On these catalysts, C–H bond activation appears to occur on the carbon support and H-adatoms are removed by Pt sites that catalyze their recombinative desorption to form H_2.

The requirement for both basic oxygen anions and acidic protons in OH groups for dehydration of alcohols to alkenes on amphoteric oxides such as Al_2O_3, which contain basic oxygens, acidic hydroxyls and Al cation sites, was proposed by Knozinger et al. [13] to explain the trans-elimination of water and the preferential formation of *cis*-2-alkenes. Basic surface oxygens interact with protons in alkanols, while protons in surface hydroxyl groups interact with the oxygen atom in the alkanol. Tanabe et al. later suggested that the unique catalytic properties of ZrO_2 in dehydration reactions arise from the presence of weak acidic

and basic sites on the surface [14–18]. In this proposal, Zr^{4+} cations act as Lewis acids that stabilize anionic species formed during hydrogen abstraction by basic oxygen sites. Such site pairs may include metal cations with orbitals accessible for coordination of adsorbed molecules. These site pairs appear to be involved also in the dissociation of H_2 in alkene and diene hydrogenation and in H_2–D_2 exchange reactions on MgO [15,19], Cr_2O_3 [20] and ZrO_2 [14,15].

4. Bifunctional reaction pathways involving acid–base site pairs

4.1. *Hydrogenation–dehydrogenation and dehydration reactions on metal oxides*

The catalytic properties of amphoteric oxides with weak acid–base site pairs often differ from those of oxides with stronger basic or acidic sites. For example, the exchange of isopropyl-d_8 alcohol with OH surface groups occurs readily on ZrO_2 at low temperatures, but not on more acidic alumina and silica–alumina catalysts [15]. ZrO_2 [21] and ThO_2 [22] catalyze the dehydration of 2-butanol to 1-butene with high (> 90%) selectivity, suggesting the involvement of anionic carbon species. In contrast, Al_2O_3 leads to the formation of 2-butenes (> 70% selectivity) [21]. On ZrO_2, 2-butanol dehydration is inhibited reversibly by the addition of either a base (*n*-butylamine) or an acid (CO_2) to the reaction mixture [21]. It appears that C–H bond activation requires not only a basic oxygen for proton abstraction, but a site capable of stabilizing the anionic product of C–H bond activation steps (Scheme 3).

This role of acid–base site pairs is similar to the stabilizing effect of solvent molecules in homogeneous acid–base catalysis. On surfaces, this stabilizing effect is provided by interactions of carbanionic intermediates with the conjugate (Lewis) acid of the basic surface oxygens or via hydrogen bonding with neighboring surface OH groups. Strongly basic oxides, with much weaker conjugate acids, or strongly acidic oxides, with weak conjugate bases, are unable to activate C–H bonds in hydrocarbons and alcohols or to dispose of the products of this reaction during a catalytic cycle.

These catalytic properties of amphoteric oxides are generally very sensitive to their thermal history, which establishes the surface density of hydroxyls, oxygen anions, oxygen vacancies, and coordinatively unsaturated cations. For example, the rate of hydrogenation of 1,3 butadiene on ZrO_2 reaches a maximum when samples are evacuated at 873 K before catalytic tests [14]. After such treatments, the rate of H_2–D_2 exchange also reaches a maximum value. This behavior is consistent with a rate-determining H_2 dissociation step in butadiene hydrogenation catalytic sequences. This step appears to occur on site pairs consisting of oxygen anions (Bronsted bases) and coordinatively unsaturated Zr cations (Lewis acids), which are required for the activation of butadiene and H_2. These site pairs are similar to those required for the selective hydrogenation of aromatic acids and discussed below.

Acid–base bifunctional effects have also been proposed in the intramolecular dehydration of monoetha-

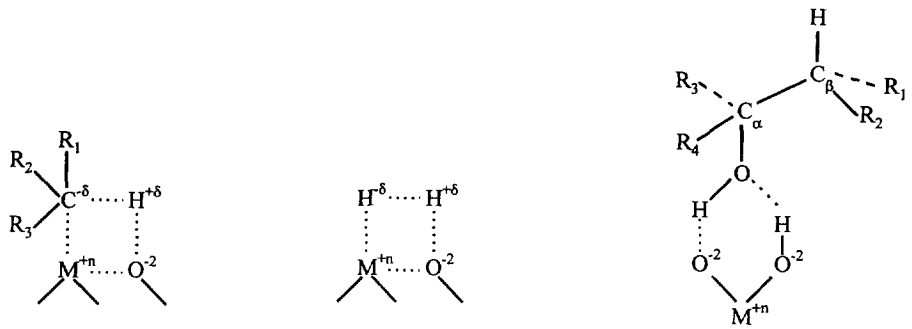

Scheme 3. Activation of C–H [3,4,31], H–H [32] and O–H [13] bonds on metal oxides.

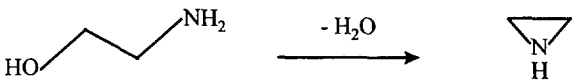

Scheme 4. Intramolecular dehydration of methanolamine to ethylenimine [23].

nolamine to ethylenimine (Scheme 4) catalyzed by SiO_2 modified by Al, P, or Ti and by alkali ions [23]. On basic oxides, such as CaO and MgO, ethylenimine selectivity was very low and the predominant reaction products were acetaldehyde and NH_3. On acidic oxides, such as TiO_2, SiO_2–Al_2O_3, and even SiO_2, the preferred reactions were intermolecular condensations to form piperazine and its derivatives. The addition of alkali, specifically Cs or Na, to SiO_2 or $SiP_{0.08}O_{2.2}$ leads to very high yields of ethylenimine. For example, methanolamine reactions on $Cs_{0.1}SiP_{0.08}O_{2.25}$ at 647 K and 0.05 bar reactant pressure lead to 79% ethylenimine selectivity at 70% reactant conversion [23]. The most effective catalytic solids for intramolecular condensation reactions desorbed NH_3 and CO_2 near room temperature. Infrared studies of the interactions of methanolamine with $Cs_{0.1}SiP_{0.08}O_{2.25}$ suggest that Bronsted acid sites protonate the amine group and a Lewis acid–Bronsted base pair abstracts a proton from the OH group in methanolamine, via bifunctional mechanisms previously proposed for alcohol dehydration [3,4], followed by ring closure and water elimination.

4.2. *Selective hydrogenation of aromatic acids to aldehydes*

Aromatic aldehydes useful as fine chemicals are typically produced by low-yield substitution reactions using halogenated intermediates. Direct reaction of H_2 with aromatic acids on Cu/Cr_2O_3 catalysts leads to complete hydrogenation to form alcohols. Selective hydrogenation of aromatic acids on TiO_2 catalysts requires the use of formic acid as the hydrogen source. Recently, Yokoyama et al. [24] have reported on the selective hydrogenation of benzoic acid to benzaldehyde using H_2 as the hydrogen source on ZrO_2 treated in air at 873 K. At 623 K, 97% selectivity to benzaldehyde was obtained at about 50% benzoic acid conversion (Table 1). Reaction rates and selectivity were highest on ZrO_2 samples with significant uptakes, but low desorption temperatures for both NH_3 and CO_2. These results suggest that weak acid and base sites are both required for selective hydrogenation reactions. Stronger acid sites appear to lead to loss of selectivity by decarboxylation of surface intermediates to form benzene and CO_2.

The addition of small amounts of metal cations such as Cr and Mn ($M_{0.05}ZrO_2$) increases reaction rates, primarily because of their stabilizing effect on ZrO_2 surface area (Table 1). Reaction rates appear to be limited by the dissociation of hydrogen, which is rapidly consumed in surface hydrogenation steps. This leads to low surface hydrogen concentrations and to

Table 1
Hydrogenation of aromatic acids to aldehydes on metal oxides [24] (625 h^{-1} H_2 space velocity; 0.02 bar benzoic acid, 0.98 bar H_2)

Catalyst	Temperature (K)	Benzoic acid conversion (%)	Benzaldehyde selectivity (%)
γ-Al_2O_3	713	20	53
MgO	713	62	4
TiO_2	713	15	10
ZrO_2	673	53	97
ZnO	673	55	54
Modified ZrO_2			
ZrO_2	623	51	97
$Pb_{0.05}ZrO_x$	583	89	96
$In_{0.05}ZrO_x$	603	100	91
$Cr_{0.05}ZrO_x$	623	98	96
$Mn_{0.05}ZrO_x$	623	70	97
$Ca_{0.05}ZrO_x$	623	50	98

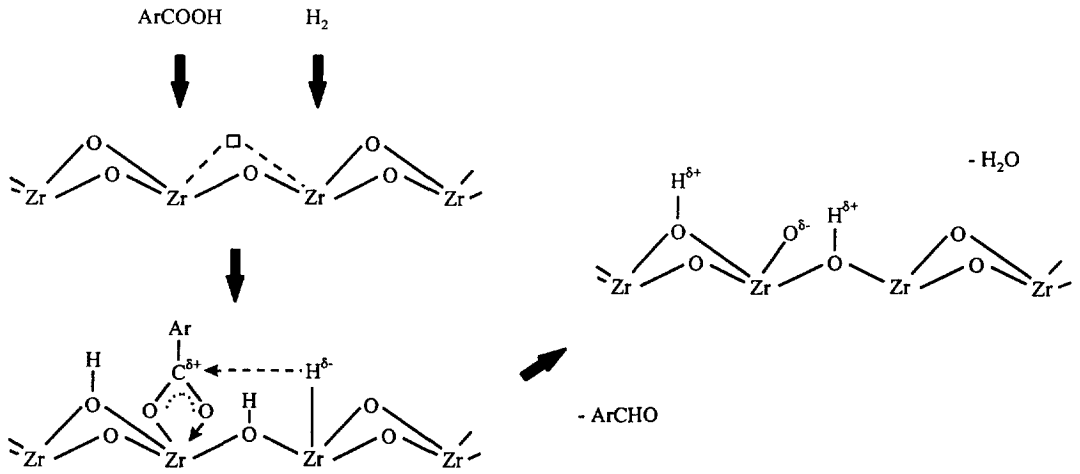

Scheme 5. Hydrogenation of aromatic acids on ZrO_2 surfaces [24].

limited hydrogenation of aldehydes to alcohols in subsequent reactions. $Cr_{0.05}ZrO_x$ catalysts lead to 96% benzaldehyde selectivity at 98% benzoic acid conversion. These materials also catalyze the hydrogenation of aliphatic, substituted aromatic, and other organic acids with very high (> 90%) aldehyde selectivity [24].

These authors have proposed a mechanism involving the dissociation of the OH group in aromatic acids and of H–H bonds in H_2 on site pairs consisting of basic oxygens and Zr^{4+} unsaturated sites associated with oxygen vacancies (Scheme 5). The reaction of hydrogen adatoms ($H^{-\delta}$) with carbon atoms in enolate-type intermediates leads to the desorption of aldehydes with the subsequent condensation of hydroxyl groups to re-form basic oxygen sites and coordinatively unsaturated Zr ions. Metal cations are known to stabilize the surface area of ZrO_2, but may also influence the density of surface vacancies and the rate-limiting H_2 dissociation steps on ZrO_2 surfaces.

4.3. *Condensation reactions on metal oxides*

Condensation reactions of alcohols, aldehydes and ketones occur on basic oxides, such as MgO and CaO, with selectivity patterns characteristic of base-catalyzed aldol condensation reactions [25]. The initial step involves the abstraction of a hydrogen atom at the α-position to the carbonyl group to form an anionic enolate-type ion. This step is followed by condensation with another molecules containing a carbonyl group, and by elimination of water from the resulting aldol species to yield α–β unsaturated compounds. Two features of these reactions suggest the requirement for a second function beyond the Bronsted base provided by oxygen anions in MgO. Aldehyde condensation reaction rates are inhibited by both CO_2 and pyridine [26] and transition metal cations strongly influence the rate of alcohol condensation reactions [27–29].

The rate of condensation of benzaldehyde to form benzyl benzoate on MgO and CaO decreases markedly when pyridine is introduced along with reactants [26]. Pyridine appears to titrate Lewis acids that are involved in rate-determining reaction steps, probably involving C–H bond activation and hydrogen abstraction. Such Lewis acid sites, consisting of coordinatively unsaturated Mg or Ca cations, bind benzylate anions formed during deprotonation of benzaldehyde. A similar bifunctional acid–base mechanism was proposed to describe the catalytic condensation of formaldehyde with acetic anhydride to form acetic and methacrylic acids on V–P–Si oxides [30]. Solids with high densities of binding sites for both CO_2 and NH_3 appear to be required for high condensation rates and selectivity. Strong acidity or basicity, characterized by the requirement for high temperatures to desorb CO_2 or NH_3, led to low reaction rates and selectivity.

The Guerbet synthesis is a type of condensation reaction involving primary or secondary alcohols, where at least one of the reactants contains a methylene group at the α-position. Ueda et al. [27–29] have reported that reactions between methanol and ethanol on MgO lead to high selectivity to 1-propanol and 2-methyl-1-propanol, the products expected in classical base-catalyzed aldol condensation pathways. The addition of Mn, Cr, or Zn cations (3–15% wt.) to MgO increased reaction rates and selectivity. In contrast, the addition of alkali, which increases the basicity of oxygen anions in MgO, decreases condensation rates. Reactions rates appear to be limited by the activation of C–H bonds in methanol because the rate of condensation of methanol with $C_nH_{2n+1}OH$ was independent of alcohol chain length [29]. Kinetic isotopic effects confirmed the rate-determining nature of the C–H bond activation step. Deuterium isotopic tracer studies are consistent with presence of both hydridic and protonic forms of hydrogen during condensation reactions on MgO. Condensation rates are not proportional to the density of basic sites measured by CO_2 chemisorption, but appear to correlate with the ability of a solid to catalyze the dehydration of isopropyl alcohol, a reaction requiring acid–base site pairs.

The more general condensation reaction between methanol and RCH_2Z molecules, where Z is an electron withdrawing group, such as –CN, –OOR, or –C_6H_5:

$$R-CH_2-Z+CH_3OH \rightarrow CH_2=\underset{\displaystyle R}{\overset{\displaystyle |}{C}}-Z + H_2 + H_2O$$

also benefits from the presence of transition metal cations on MgO catalysts [27]. For example, the rate of the reaction between methanol and acetonitrile increases by a factor of ca. 100 when MnO species are present on the surface of MgO [27]. The selectivity to acrylonitrile is 96% at reaction temperatures of 623 K. Mn-promoted MgO also catalyzes the reaction of methyl-propionate with methanol to give methyl methacrylate with 60% selectivity.

These results suggest that C–H bond activation steps required for condensation reactions on basic oxides also require cationic metal centers to stabilize carbanionic intermediates. While coordinatively unsaturated Mg cations can play this role in MgO, the presence of a more reducible or accessible cation increases the density and strength of such Lewis acid sites.

4.4. *Acid–base site requirements in deuterium exchange reactions*

H_2–D_2 equilibration and hydrocarbon exchange with gas phase D_2 or with surface OD groups also depend on the acid–base properties of metal oxides and on the presence of hetero-cations that can form H adatoms from H_2. Hoq and Klabunde [31] have shown that the exchange between hydrocarbons (RH) and D_2 on MgO (dehydrated at 933 K) depends on the solution phase acidity of the C–H groups in RH. This suggests that exchange occurs via a concerted mechanism involving a Bronsted base (oxygen anions) to abstract $H^{+\delta}$ and a 'solvent' effect by Mg^{+2} or other charged centers to stabilize the $R^{-\delta}$ in the products and in the transition state for exchange. This bifunctional catalytic behavior thus depends on solution-phase rather than gas phase acidities. The participation of the cationic center in Mg-O site pairs is also consistent with the infrared observation of $H^{-\delta}$ species associated with cationic centers and $H^{+\delta}$ in surface hydroxyl groups in ZnO, MgO, SrO, and CaO [32]. These site pairs appear to exist as low-coordination anion–cation couples on high surface area oxides [36]. These low-coordination sites allow the stabilization of $H^{-\delta}$ and $H^{+\delta}$ to be shared by several anions and cations.

Boudart et al. [19] have shown that H_2–D_2 equilibration occurs at 77–273 K with very low activation energy (2.1–2.3 kcal/mol). Reaction rates reach a maximum after dehydration of MgO at about 800 K and decrease rapidly after dehydration at higher temperatures or after exposure to H_2O at temperatures leading to MgO surface restructuring. These authors have proposed that equilibration requires MgO(111) surface planes, which contain OH groups and electronic defects consisting of electron-deficient paramagnetic centers.

Butadiene deuterogenation, however, occurs with high selectivity on MgO samples evacuated at 1373 K without detectable H_2–D_2 equilibration [15]. The predominant *cis*-2-butene product contains intact two deuterium atoms, located at opposite ends of the molecule, suggesting that dissociation occurs before deuterogenation. These data suggest that dehy-

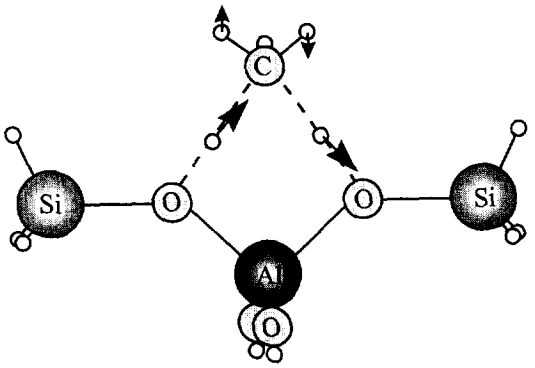

Scheme 6. Proposed transition state geometry in exchange reactions of CD_4 with OH groups in aluminosilicates [33].

dration at high temperatures may inhibit the migration of hydrogen adatoms on MgO, a step that is required in H_2–D_2 equilibration. The loss of OH groups after high temperature treatments may isolate dissociated D–D pairs on the surface, which may still react with physisorbed or π-bonded butadiene by addition of D^{-6} to form allylic carbanions.

Another example of the 'solvating effect' of acid–base pairs in exchange reactions was recently provided by experimental and theoretical studies of the interaction and exchange of CD_4 with OH groups in aluminosilicates [33,34]. The calculated transition state geometry for this exchange process (Scheme 6) shows a concerted interaction of the carbon in methane with the H in acidic OH groups and one hydrogen atom in methane with a basic framework oxygen. This species is covalently bonded to the surface and the activation barrier for its formation is determined by acidity differences between proton accepting and donating sites [33]. This concerted interaction of an alkane with an acid–base surface pair is also likely to play a critical role in alkane C–H bond activation on zeolites. For example, interactions of additional H atoms with basic oxygens, which are not possible in the small clusters used for the calculation of the transition state structures in Scheme 6 [33], may lead to recombination to form H_2, or for larger alkanes, to the formation of methane by 'hydride' addition at the end of adsorbed hydrocarbons.

The promotional effect of cations or metal clusters on the rate of exchange between gas phase D_2 and surface OH groups in zeolites [35] show that rapid surface migration of H atoms occurs at typical catalytic temperatures. In effect, H atoms in structures such as Scheme 6 or in unperturbed OH groups are able to exchange with H-atoms formed by dissociative adsorption on distant H_2 dissociation sites. Consequently, we must consider the possibility that the surface-coordinated H-atoms in Scheme 6 can diffuse to distant recombinative desorption sites, thus allowing the interaction of another H atom in adsorbed species with framework oxygen sites during one alkane surface sojourn. Exchange occurs when the C–H activation reaction is reversed chemically but not isotopically. Dehydrogenation and formation of alkoxide-type species occur when C–H activation steps become irreversible as one of the coordinated H-atoms in Scheme 6 is removed by diffusion to and recombinative desorption on cationic or metal sites. This allows adsorbed intermediates to recycle basic framework oxygen sites for sequential hydrogen abstraction steps leading to C_nH_{2n+1}–O species, at least for propane and larger alkane reactants. These concepts will become relevant in Section 7.1, in the context of unconcerted bifunctional pathways for the activation and dehydrogenation of propane on cation-exchanged H-ZSM5.

5. Stoichiometric and catalytic reactions of probe molecules for the characterization of acid and base sites

The ubiquitous role of multifunctional pathways in catalysis by acids and bases complicates the structural and mechanistic characterization of specific surface species using stoichiometric and catalytic reactions of probe molecules. For example, it appears that both acid and base sites are involved in dehydration of alcohols [4,13], a reaction frequently used to detect the presence of acid sites on heterogeneous catalysts. Also, alcohol condensation and dehydrogenation reactions, normally associated with basic sites, appear to benefit from the presence of Lewis acids that stabilize the anionic product of hydrogen abstraction steps [26–29]. Both types of reactions are inhibited by the presence of basic (pyridine or NH_3) and acidic (CO_2) molecules in the gas phase. In some cases, Lewis acid sites are provided by coordinatively unsaturated cations in monometallic oxides, the surface density of which depends sensitively on dehydration

temperatures. In other cases, a second element, either as part of a single phase binary oxide or as a separate well-dispersed oxide phase, provides coordinatively unsaturated cations for the stabilization of carbanion intermediates.

Bronsted acid sites can be probed by reactions involving 'protonation' of molecules with π-bonds. For example, reactions of alkenes on aluminosilicates involve proton transfer to the alkene and stabilization of adsorbed carbocations via electron donation from the conjugate base consisting of oxygen atoms in acidic hydroxyls [36]. These simple acid-catalyzed reactions involve oxygen atoms acting as a conjugate base. They have been described as bifunctional reactions, even though the basic function merely replaces a role normally played by the solvent in homogeneous acid–base reactions. This process leads to covalently bonded alkoxy-type species that nevertheless retain carbocationic character in the transition state and, thus, follow the rules for reactions of protonated hydrocarbons [36].

The isomerization of 2-methyl-2-pentene, pioneered by McVicker et al. [37], probes the residence time of these adsorbed intermediates by observing the probability that desorbed molecules have undergone double-bond shift, methyl shift, or 'chain lengthening'. Weakly adsorbed intermediates with short residence times desorb either unreacted or after facile hydride shifts leading to the migration of double bonds. Methyl shifts along the molecule backbone also involve a shift in the location of the molecule-surface linkage from a secondary to another secondary carbon and requires longer surface residence times than hydride shifts. Finally, chain lengthening involves the shift of a backbone methyl chain to the end of the molecule and the formation of surface bonds with less coordinated carbons. It occurs only when desorption (deprotonation) processes are slow, a situation normally associated with strongly bound intermediates. Thus, 2-methyl-2-pentene isomerization reactions favor the formation of linear hexenes only for Bronsted acid sites that interact strongly with surface intermediates. Very strong acids, however, lead to long surface residence times, which also favor chain growth via alkylation reactions and permanent attachment of adsorbed species, which lead to irreversible deactivation and to kinetically invisible strong acid sites.

Catalytic probe reactions on basic sites generally involve the initial abstraction of a proton from a molecule and the formation of adsorbed carbanions. These carbanions must be stabilized by interactions with a Lewis acid site, such as a coordinatively unsaturated cation. In many cases, such cations are sterically hindered and become available for interactions with adsorbed species only at surface steps or near oxygen vacancies. As a result, it is likely that many base-catalyzed reactions probe the basicity of oxygen anions only indirectly during C–H or O–H bond activation steps, because the concerted nature of these steps and the resulting carbanion–cation interactions make the strength of the latter relevant to the activation energy for C–H or O–H bond activation steps. Thus, in general, base-catalyzed reactions probe the properties of acid–base pairs. Condensation reactions of acetone (Scheme 7) may provide an indirect but useful probe of basic sites. The stability of the surface enolate species formed in α-hydrogen abstraction steps make it likely that reaction rates will depend primarily on the stability of the O–H bond formed and thus on the basicity of the metal oxide. Reactions of acetone, aldehydes and alcohols on base oxides, however, may depend sensitively on the presence of cations and H_2 adsorption–desorption sites. It appears that most of these reactions probe to some extent a balance between the basicity of the oxygen anions and the ability of the balancing cation to accommodate the products of proton abstraction steps.

Lauron-Pernot et al. [38] have recently used reactions of 2-methyl-3-butyn-2-ol as a diagnostic tool to determine the densities of acid and base sites and of acid–base site pairs in metal oxides. The observed reaction pathways of this tertiary alkynol are shown in Scheme 8. Base oxides, such as MgO and ZnO, lead to the exclusive formation of acetylene and acetone via intramolecular hydrogen transfer. This reaction is likely to involve the dissociation of O–H bonds in acid–base site pairs and attack by protons at electron-rich triple bonds in the acetylenic end of the molecule. This type of 'hydrogenation' reaction is characteristic of ZnO and MgO, which hydrogenate dienes at relatively low temperatures. Bronsted acids, such as SiO_2–Al_2O_3, lead preferentially to dehydration to form methyl-butyne and 3-methyl-but-3-ene-1-yne. Amphoteric oxides, such as Al_2O_3, lead to the formation of two new products: hydroxybutanone and

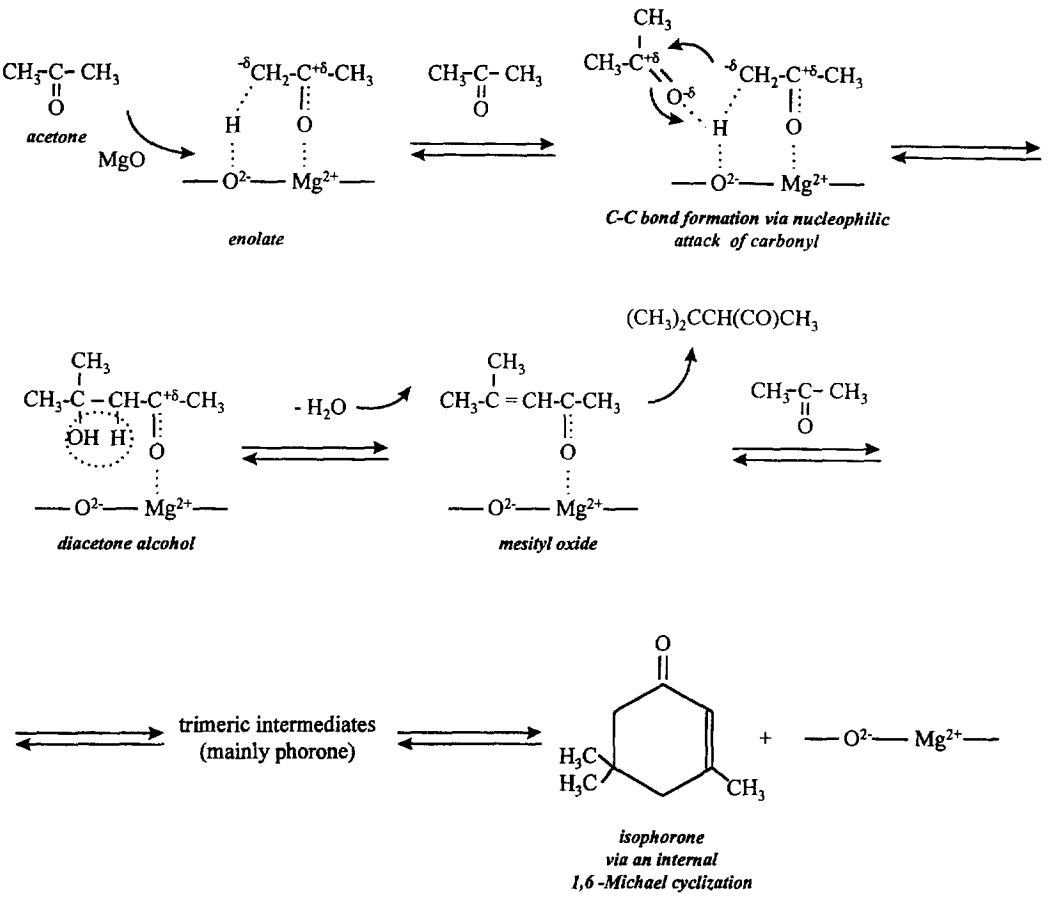

Scheme 7. Reactions of acetone on base oxides.

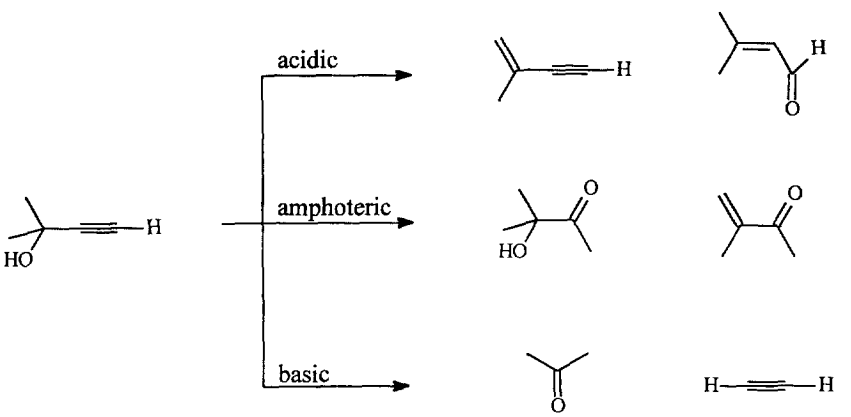

Scheme 8. Reactions of 2-methyl-3-butyn-2-ol on acid, base, and amphoteric oxides [38].

methyl-isopropyl ketone. ZrO_2 leads to the formation of hydroxybutanone with 76% selectivity. The formation of hydroxybutanone requires hydration of the tertiary alkynol reactant, but water is available only as it is formed in parallel dehydration reactions. Thus, the high hydroxybutanone selectivity observed on ZrO_2 must arise in part from a stoichiometric reaction with surface hydroxyl groups on ZrO_2. The mechanism of these reactions remains unclear. This example, however, demonstrates the complexity of molecular structures and reaction pathways required in order to probe multi-functional surfaces. One should consider, at this level of complexity, the usefulness of the probe molecule reactions in comparison with a direct study of the mechanism and structural requirements for the specific reaction of practical interest.

The titration of acid and base sites with molecular acids and bases has been widely used to count the number of surface sites on metal oxides. In addition, temperature-programmed desorption and calorimetric methods are frequently used in order to estimate the desorption activation energy or the enthalpy of the titration reaction. Recently, Tanabe [17] has proposed the use of phenol as a titrant of acid–base site pairs. Phenol can dissociate on acid–base pairs near room temperature, but in contrast with aliphatic alcohols cannot undergo dehydration or dehydrogenation reactions during temperature-programmed desorption studies. Therefore, desorption occurs by recombination of surface species to re-form phenol molecules. Recombinative desorption of hydrogen atoms before desorption, however, may isolate adsorbed phenolic species on such bifunctional surfaces and lead to incomplete desorption of adsorbed phenol.

Exchange reactions between hydrocarbons and OD groups on Bronsted acid surfaces appear to depend also on the corresponding basicity of the conjugate basic oxygens [31,32]. These reactions are useful probes of the reactivity and density of protons and of the role of the conjugate base in the activation of C–H bonds involved as the rate-determining step in many reactions of practical interest. Exchange reactions appear to be particularly useful probe reactions because they probe elementary reaction steps without requiring stoichiometric chemical reactions. Isotopic transient methods using acidic, basic, or amphoteric molecules provide a useful complement to other probe reactions by determining the adsorption–desorption properties of metal oxide surfaces at constant temperatures and coverage. Our group has recently used successfully a $^{13}CO_2$–$^{12}CO_2$ isotopic switch method for the characterization of basic sites in modified MgO catalysts useful in alcohol condensation reactions [39].

Titration of acid sites is most effective when the titrant interacts weakly with the surface site and when the structure of the adsorbed species is followed by spectroscopic methods. In this regard, infrared studies of weakly adsorbed H_2 [40], N_2 [41] and CO [42] on metal oxides below room temperature have been extremely useful in establishing the density and type of Lewis and Bronsted acid sites on oxide surfaces.

Titration and catalytic reactions of probe molecules are often used as indirect measures of the number of sites or the reaction rate for a different reaction of specific interest. Ultimately, these probe molecule methods will be replaced by more direct and specific techniques that measure the concenration and reactivity of intermediates as the catalytic reaction of interest proceeds. Recent applications of these in-situ methods include isotopic switch studies [43], dynamic infrared spectroscopy [44] and in-situ X-ray absorption spectroscopy [45].

6. Bifunctional dehydrogenation–acid pathways on WC modified by chemisorbed oxygen

Bifunctional pathways discussed in the previous sections require that two sites co-exist within molecular distances and act in a concerted manner on a reaction step. Such sites and pathways can be decoupled spatially, but remain coupled kinetically when rapid gas phase diffusion transfers intermediate species between the two sites. In most cases, this is accomplished by placing crystallites with one type of site onto a support that contains the second site. Here, we discuss the behavior of WC_x catalysts modified by chemisorbed oxygen, in which a monofunctional surface becomes bifunctional through a local transformation of surface regions by contact with oxygen.

Tungsten carbides (WC) prepared by isothermal carburization of WO_3 or W_2N with CH_4/H_2 mixtures catalyze *n*-alkane hydrogenolysis and methylcyclohexane dehydrogenation with high selectivity [46–49]. Bifunctional pathways are introduced by the

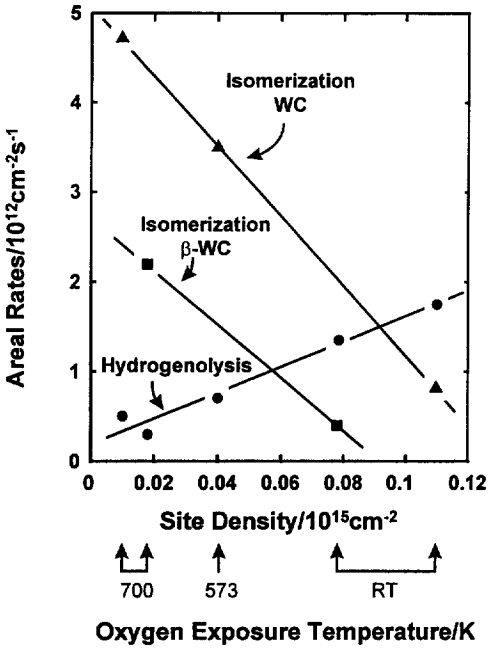

Fig. 1. *n*-Hexane isomerization on tungsten carbides modified by chemisorbed oxygen.

presence of chemisorbed oxygen on WC_x carbide surfaces, apparently by the formation of Bronsted acid sites on WO_x species using hydrogen atoms formed in H_2 dissociation or C–H bond activation steps catalyzed by WC_x sites [46,47,50]. For example, *n*-hexane hydrogenolysis (and dehydrogenation) rates are proportional to the number of WC_x sites counted by CO titration methods (Fig. 1). The conversion of these WC_x sites to WO_x sites by controlled contact with O_2 inhibits hydrogenolysis rates, but increases markedly the rate and selectivity of *n*-hexane conversion to branched isomers (Fig. 1). Isotopic tracer studies have shown that this reaction proceeds via quasi-equilibrated dehydrogenation steps followed by rate-determining isomerization steps [47]. The products of 3,3 dimethyl-pentane isomerization are consistent with a methyl-shift mechanism typical of acid-catalyzed isomerization steps [47]. The rate of *n*-hexane isomerization was proportional to the density of oxygen atoms present on oxygen-modified WC surfaces, suggesting that WO_x are responsible for Bronsted acidity. Methylcyclohexane converts exclusively to toluene on WC, but acquires ring isomerization pathways leading to alkyl-cyclopentanes when oxygen atoms are placed on the surface [47]. The isomerization pathways involve methylcyclohexene intermediates and rate-determining isomerization steps on acid sites consisting of surface WO_x species.

These bifunctional catalysts are unique in two important aspects. They become bifunctional through an incomplete oxidation process that permits the coexistence of 'reduced' and 'oxidized' surface species. Also, Bronsted acid sites form only when a complementary site is available in order to produce the H-atoms required for the conversion of WO_x into protonic WO_x–H species [50]. As we discuss later, the formation of protonic sites via hydrogen spillover from H_2 or C–H dissociation sites appears to be quite prevalent in acid–base catalysis when H_2 activation occurs on metal sites or reducible cations on oxide surfaces. The resulting bifunctional pathways are described in the examples of the next section.

7. Kinetic coupling between hydrogen activation and acid–base functions in C–H activation reactions

In many cases, the two functions required to complete a catalytic sequence must reside within molecular distances in order to act upon an elementary step in a concerted manner and thus decrease its activation barrier. In general, however, a second catalytic site can be separated spatially beyond molecular distances and remain effective in bifunctional pathways, but only if the two sites communicate by surface or gas phase diffusion within the time scale of a catalytic turnover. Then, the two sites are able to couple kinetically separate elementary steps or catalytic sequences within a complex reaction scheme. Bifunctional hydroisomerization and reforming reactions become possible because alkenes diffuse through intrapellet voids between dehydrogenation sites, where they are formed, and acid sites, where they undergo skeletal transformations [9,10]. Such bifunctional pathways remain effective even when the functions become separated by macroscopic distances (0.01–0.1 mm) [10]. In this section, we discuss bifunctional pathways in which hydrogen adsorption–desorption sites and acid or base sites communicate by rapid surface diffusion of hydrogen. In this manner, C–H bond activation steps and hydrogen introduction or removal

become kinetically coupled and overcome a rate-determining step within a hydrogenation–dehydrogenation catalytic sequence.

A second site influences an otherwise monofunctional step with positive standard Gibbs free energy (negative standard affinity) by coupling it kinetically with a favorable elementary step. This new (or parallel) step either removes the products or increases the surface concentration of the reactants involved in the unfavorable step [51]. Propane dehydrogenation reactions on H-ZSM5 modified by Zn cations, *n*-heptane isomerization on zirconia modified by WO_x (or SO_x) and Pt, and alcohol condensation reactions on Cu-promoted Mg_5CeO_x oxides provide useful examples of the role of kinetic coupling between hydrogen adsorption–desorption 'portholes' [52,53] and acid or base sites in catalytic reactions involving the activation of C–H bonds. In each case, sites introduced by metal crystallites (Pt, Cu) or by isolated cations (Zn^{2+}) increase the rate of reactions typically occurring on acid or base sites by introducing a 'porthole' for adsorption–desorption reactions of H_2. These bifunctional pathways appear to avoid the need for unsaturated gas phase intermediates such as alkenes or aldehydes, which are not favored by thermodynamics at low temperatures or high H_2 pressures. These catalytic sequences require, however, the activation of C–H bonds on acid or base sites, the formation of mobile surface hydrogen species and their migration on surfaces to hydrogen activation and desorption sites.

7.1. *Catalytic dehydrogenation reactions of alkanes on cation-modified H-ZSM5*

Propane conversion to alkenes and aromatics on cation-modified H-ZSM5 requires sequential dehydrogenation steps followed by chain growth and cyclization reactions of propene intermediates [45,54]. Reaction rates on H-ZSM5 increase markedly when some of the protons are exchanged with Zn or Ga cations (Table 2). Cations must be located at exchange sites in order to maximize their beneficial effect on dehydrogenation rates and selectivity and to prevent their elution from the catalyst as metal vapors at typical reactions conditions.

Dehydrogenation reactions proceed via elementary steps that require the activation of C–H bonds in alkanes and the disposal of the H-atoms formed in these reactions. The rates of C–H activation, recombinative hydrogen desorption and propane dehydrogenation were measured simultaneously from isotopic redistribution and chemical conversion data using C_3H_8/C_3D_8 and D_2/C_3H_8 mixtures [45,54,55].

Table 2
Aromatics turnover rate and selectivities on H-ZSM5, 2.1% Ga/H-ZSM5, and 1.3% Zn/H-ZSM5 (773 K, 26.6 kPa C_3H_8, balance He, 8.6–9.6% propane conversion, Si/Al = 14.5)

	H-ZSM5	Ga/H-ZSM5	Zn/H-ZSM5
Aromatics turnover rate (per Al, 10^{-3} s^{-1})	0.1	2.3	1.8
Carbon selectivity (%)			
C_1–C_2	62.3	29.3	25.8
Propene	24.9	30.8	32.9
C_{6+} aromatics	3.9	31.2	35.8
Hydrogen selectivity (%)			
Hydrogen (H_2)	6.0	26.7	30.5
C_1–C_2	66.7	29.2	26.2
C_{6+} aromatics	1.6	13.0	14.8

C–H bond activation rates measured from isotopic scrambling rates in C_3H_8/C_3D_8 mixtures are similar on H-ZSM5, Zn/H-ZSM5 and Ga/H-ZSM5 and negligible on Na/ZSM5, suggesting that C–H activation occurs predominantly on Bronsted acid sites (Table 3). In contrast, dehydrogenation rates vary by more than a factor of ten among these catalysts. Isotopic scrambling rates are much faster than the rate of propane conversion to aromatics, a complex

Table 3
Overall propane conversion turnover and C–H bond activation rates on H-ZSM5, 2.1% Ga/H-ZSM5, 1.0% Zn/H-ZSM5, 1.3% Zn/H-ZSM5 and Na-ZSM5 (from cross exchange rates of C_3H_8/C_3D_8 mixtures) (773 K, 6.6 kPa C_3H_8, 6.6 kPa C_3D_8, balance He, Si/Al = 14.5)

	Propane conversion turnover rate per Al site (10^{-3} s^{-1})	C–H bond activation turnover rate per Al site (10^{-3} s^{-1})
H-ZSM5	0.3	32.2
2.1% wt. Ga/H-ZSM5	4.0	38.2
1.0% wt. Zn/H-ZSM5	2.9	62.2
1.3% wt. Zn/H-ZSM5	4.3	70.8
Na-ZSM5	$\ll$0.1	1.6

sequence of reactions controlled by the rate of the initial propane dehydrogenation reaction. C–H bond activation steps occur rapidly even on protonic acid sites, but they are quickly reversed by recombination of hydrocarbon fragments with abundant surface hydrogen species, because such sites are not able to remove hydrogen via recombinative desorption. Zn and Ga cations prevent these recombination reactions by providing a function for recombinative desorption and removing the hydrogen atoms formed during C–H activation, as first proposed by Mole et al. [56]. Exchanged Zn and Ga cations increase the rates of propane aromatization (Tables 2 and 3) by increasing the rate of recombinative desorption of the hydrogen atoms formed in C–H activation steps. In effect, C–H bond activation steps that can occur with some difficulty on acid sites because of unfavorable reaction affinities become coupled with recombinative desorption on a separate site. These sites communicate with acid sites via rapid migration of H-atoms from momentary adsorption sites in the vicinity of Bronsted acid sites to Lewis acid sites provided by exchanged metal cations.

This proposal is consistent with the effects of Zn (and Ga) cations on the rate of H_2–D_2 isotopic exchange (Fig. 2) and with the rate of incorporation of D-atoms from D_2 into the products of C_3H_8–D_2 reactions (Fig. 3). In addition, competitive reactions of 2-^{13}C-propane and unlabeled propene have shown that initial dehydrogenation steps become increasingly irreversible as Zn cations deplete by recombinative desorption the surface pool of hydrogen available for the reverse hydrogenation reaction [55]. These conclusions are consistent with the results of Le van Mao et al. [57] using physical mixtures and confirm the original mechanistic proposal of Creer et al. [56]. This 'reverse spillover' of hydrogen was first observed during the decomposition of GeH_4 on a Ge film [52,53], well before the discovery [58,59] and popular acceptance [60–63] of hydrogen spillover processes on heterogeneous catalysts. Reverse spillover concepts were later used in order to describe the function of Pt clusters in dehydrogenation reactions catalyzed by carbon [12].

The initial dehydrogenation step in propane conversion to aromatics on cation-modified H-ZSM5 involves quasi-equilibrated exchange between zeolite and alkane hydrogens, a reaction mechanistically

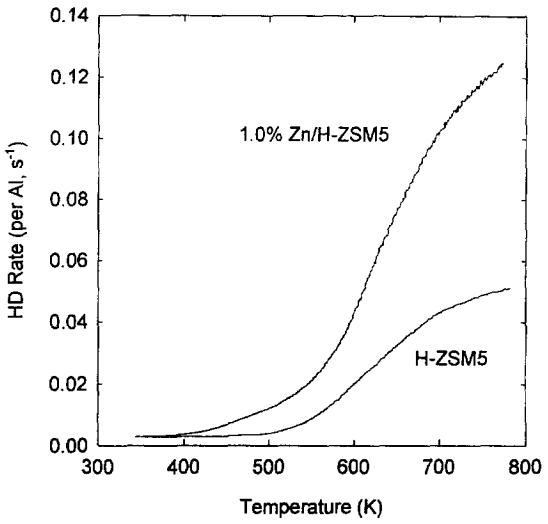

Fig. 2. H_2/D_2 exchange rates on H-ZSM5 and 1.0% Zn/H-ZSM5 as a function of temperature (15 K/min, 5% H_2, 5% D_2, 90% Ar, 100 cm^3/min, Si/Al = 14.5).

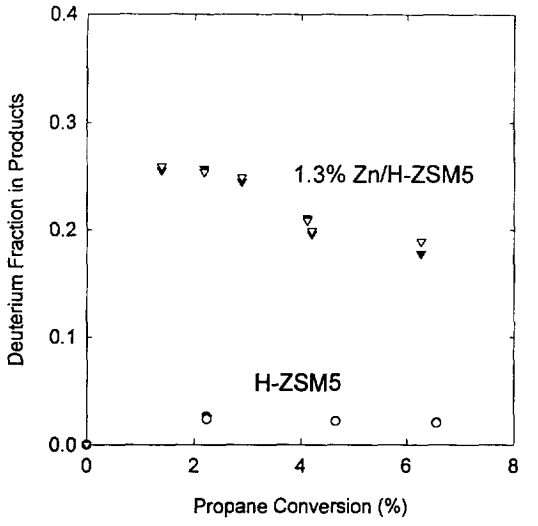

Fig. 3. Deuterium fraction in propylene and benzene of propane/deuterium mixtures on H-ZSM5 and 1.3% Zn/H-ZSM5 in a recirculating batch reactor (773 K, 26.6 kPa C_3H_8, 6.7 kPa D_2, balance He, Si/Al = 14.5).

related to C–H activation steps, and rate-determining removal of hydrogen species formed during C–H activation. Hydrogen removal can occur via bimolecular or surface-mediated transfer to adsorbed hydrocarbons (hydrogen transfer) or by recombination to

form H_2. Stoichiometric hydrogen 'acceptors', such as O_2, CO and CO_2 also increase aromatics selectivity by coupling dehydrogenation steps with hydrogen removal via hydrogenation of these molecular acceptors [45].

Rate-determining hydrogen desorption steps create high hydrogen virtual pressures [64] at catalytic surfaces and lead to unfavorable thermodynamics for surface C–H bond activation elementary steps and to 'hydrogenation' surface reactions that form predominantly light alkanes. The kinetic coupling between Bronsted acid sites provided by Al sites within zeolite channels and dihydrogen activation sites consisting of isolated Zn^{2+} cations bridging two exchange sites leads to bifunctional pathways consistent with measured kinetic rate expressions for propane conversion and with the observed correlation between dehydrogenation rates and H_2–D_2 isotopic exchange rates. The presence of exchanged Zn or Ga cations increases the rate of hydrogen removal by introducing 'portholes' [52] for the recombinative desorption of H-atoms as H_2 and decreases the rate of formation of undesired light alkanes [45,54,55].

7.2. *Isomerization reactions on Pt/WO_x–ZrO_2 and Pt/SO_x–ZrO_2*

Zirconia becomes a strong solid acid when modified by depositing WO_x [66] or SO_x [65] species on the surface of hydrous zirconium oxide. When promoted with metals (e.g., 0.3% wt. Pt), these oxides catalyze the selective hydroisomerization of S^{7+} alkanes at 373–473 K without the extensive cracking observed on sulfated zirconia and zeolites promoted by metals [67,68].

Kinetic and isotopic tracer data are not consistent with bifunctional pathways involving gas phase alkene intermediates. Instead, isomerization reactions proceed via chain reactions involving hydrogen transfer from alkanes, H_2, or hydride donors, such as adamantane, to adsorbed isomerized hydrocarbons [67,68]. Hydrogen transfer steps lead to desorption of surface intermediates and decrease the surface residence time of such species. As a result, desorption occurs before undesired C–C scission events. Hydrogen transfer occurs primarily using H-atoms formed by H_2 dissociation on metal sites in Pt/SO_x–ZrO_2 and Pt/WO_x–ZrO_2 catalysts.

Table 4
n-Heptane reactions on Pt/SO_x–ZrO_2 and Pt/WO_x–ZrO_2. Isomerization selectivity, reaction kinetics and isotopic tracer data (Catalysts: 0.3% wt. Pt, 12.7% wt. W or 4.5% wt. S)

	Pt/SO_x–ZrO_2	Pt/WO_x–ZrO_2
Isomerization selectivity (%) [a]	32	89
n-Heptane reaction order [b]	0.2	0.9
H_2 reaction order [b]	1.0	−0.5–0
Adamantane reaction order [a,c]	0.9	0.05
Deuterium content in *n*-heptane (%) [d]	6	82
Deuterium content in methylhexanes (%) [d]	80	83

[a] 473 K, 650 kPa H_2, 100 kPa *n*-heptane, 50% *n*-heptane conversion.
[b] 473 K, 800–2900 kPa H_2, 33–200 kPa *n*-heptane.
[c] 0–1.0% mol. adamantane.
[d] 343 K, 3.7 kPa *n*-heptane, 97 kPa D_2, 5% *n*-heptane conversion.

On Pt/SO_x–ZrO_2, these hydrogen transfer desorption steps are slow because Pt surface atoms become poisoned by chemisorbed sulfur. Slow desorption of adsorbed intermediates then leads to significant β-scission before desorption and to low isomerization selectivity. Isomerization rates and selectivity increase with increasing concentration of H_2 and *n*-heptane, and also when very small concentrations of adamantane are added to the reactant stream (Table 4) [67,68]. Reactions of n-C_7H_{16}–D_2 mixtures lead to complete scrambling and binomial deuterium distributions in all reactions products, but not in 'unreacted' *n*-heptane (Table 4), suggesting that desorption of intermediates is slow and occurs only after significant skeletal rearrangements have occurred. In effect, the introduction of *n*-heptane into the pool of surface intermediates, shown schematically in Scheme 9, is irreversible on Pt/SO_x–ZrO_2 catalysts, because *n*-heptane surface species seldom desorb before several surface isomerization events.

On Pt/WO_x–ZrO_2, hydrocarbon adsorption–desorption via hydrogen transfer is rapid at 473 K. *n*-Heptane adsorption–desorption is quasi-equilibrated and surface isomerization steps limit the overall reaction rate. As a result, desorption of isomerized surface species often occurs before significant β-scission on Pt/WO_x–ZrO_2. Isomerization kinetics become of the first order in *n*-heptane and of zero-to-negative order in H_2, suggesting that hydrogen transfer steps become quasi-equilibrated and cause the undesired desorption

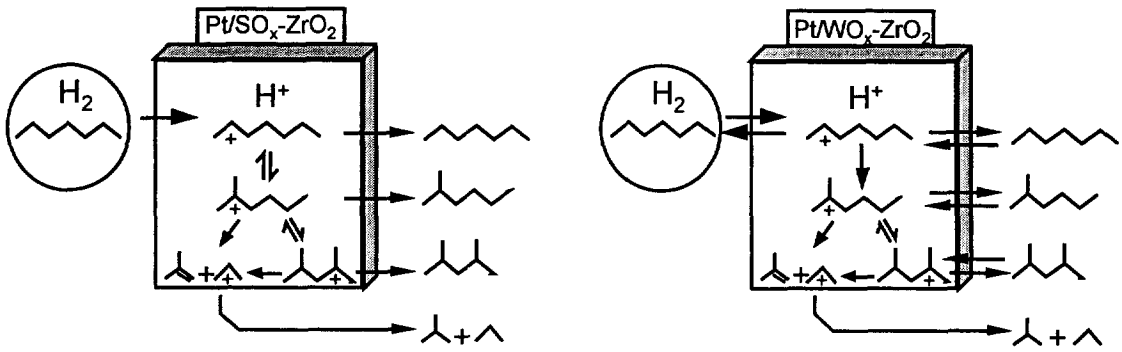

Scheme 9. Reaction pathways for bifunctional isomerization of *n*-heptane on Pt/SO_x–ZrO_2 and Pt/WO_x–ZrO_2 [65].

of intermediates before skeletal isomerization occurs (Table 4). Adamantane does not affect *n*-heptane isomerization rates or selectivity on Pt/WO_x–ZrO_2, because hydrogen transfer steps are quasi-equilibrated and, therefore, do not benefit from co-catalysts that increase the rate of such reactions. Reactions of *n*-C_7H_{16}–D_2 mixtures lead to complete scrambling and binomial deuterium distributions in 'unreacted' *n*-heptane and in all reactions products (Table 4), suggesting the reversible (quasi-equilibrated) adsorption–desorption of *n*-heptane reactants on catalytic sites. A zero-to-negative hydrogen pressure dependence reflects the frequent and undesired desorption of adsorbed intermediates (by hydrogen transfer from H_2) before isomerization occurs.

On both Pt/WO_x–ZrO_2 and Pt/SO_x–ZrO_2, hydrogen species formed by H_2 dissociation on Pt sites participate in chain termination reactions of cationic or alkoxide-like intermediates adsorbed on acid sites and in the formation of Bronsted acid sites (Schemes 10 and 11). These bifunctional reaction pathways appear to involve the spillover of hydrogen adatoms from Pt sites, onto WO_x centers, with the formation of

$$(C_7H_{15})\,(W^{+6})_{n-1}\,(W^{+5})\,O_{3n} + H\text{-}Pt_x \longrightarrow (W^{+6}\,O_3)_n + C_7H_{16}\,(g) + Pt_x$$

Scheme 10. Desorption of carbocationic species by transfer of hydrogen from Pt to WO_x sites [65].

$$H\text{-}H + (W^{+6}\,O_3)_n \rightleftharpoons (H^+)_2\,(W^{+6})_{n-2}\,(W^{+5})_2\,O_{3n}$$

Scheme 11. Formation of Bronsted acid sites on WO_x species by migration of hydrogen atoms from Pt dissociation sites.

reduced tungsten species and acidic hydrogens or tungsten bronzes (Scheme 11). As a result, hydrogen atoms formed at H_2 dissociation sites become involved not only in the desorption of hydrocarbon intermediates, but in the generation of Bronsted acid sites [68]. The formation of Bronsted acid sites during H_2 treatment has been directly observed by infrared measurements of the density of Lewis and Bronsted acid sites in Pt/SO_x–ZrO_2 by Hattori et al. [69,70], who showed that Lewis acid sites are converted to Bronsted acid sites during contact with H_2 at temperatures typical of those required for their catalytic action.

Pt/WO_x–ZrO_2 catalysts share the WO_x acid function of the bifunctional oxygen-modified WC catalysts discussed in Section 6. The hydrogenation–dehydrogenation function is provided by Pt in the former and by WC in the latter. Yet, *n*-alkane isomerization proceeds by non-concerted bifunctional catalysis leading to similar products but involving the diffusion of a different species between the two sites. On WC catalysts, alkenes act as intermediates, while on Pt/WO_x–ZrO_2 surface hydrogen species are involved. This appears to be principally the result of the much higher temperatures (623 K vs. 453–473 K) required for significant isomerization rates on WC catalysts. At these higher temperatures, equilibrium alkene concentrations are much higher and provide an effective diffusive pathway. On Pt/WO_x–ZrO_2 (at 473 K), hydrogen surface concentrations are sufficiently high to provide an alternate and more effective pathway for communication between hydrogenation–dehydrogenation and acid sites than (undetected) gas phase alkenes.

The presence of dihydrogen appears to influence acid-catalyzed reactions even in the absence of Pt sites [71]. Dihydrogen (101 kPa) increased *o*-xylene isomerization rates by a factor of four on WO_x–ZrO_2 at 523 K, suggesting the activation and involvement of H_2 on WO_x–ZrO_2 during acid-catalyzed reactions. The absence of H_2 leads to irreversible loss of active sites, apparently as the result of H_2 desorption and destruction of Bronsted acid sites during *o*-xylene reactions. Reactions of *o*-xylene/D_2 mixtures show that dihydrogen participates in the formation of Bronsted acid sites, but not in hydrogen transfer elementary steps during xylene isomerization [71]. Instead, reaction occurs by protonation–deprotonation reactions of *o*-xylene with intervening methyl shifts. These Bronsted acid sites consist of H_xWO_3 species present at the surface of small octahedral WO_3 clusters and formed by hydrogen migration from H_2 dissociation sites.

Recently, we have obtained independent evidence for the presence of spillover hydrogen and for reduced W centers. Near-edge X-ray absorption studies and temperature-programmed reduction studies have detected the reduction of W^{6+} centers during hydrogen treatment at 473–673 K [68,71]. Site titration studies using H_2, O_2 and CO show that hydrogen uptakes exceed monolayer coverages on Pt sites after H_2 treatments at typical isomerization temperatures (Table 5). CO chemisorption leads to monolayer coverage and to estimates of Pt crystallite diameters in agreement with electron microscopy measurements. O_2 uptakes are significantly higher than those of H_2 or CO, especially as reduction temperature increases, suggesting significant re-oxidation of reduced WO_x species formed during H_2 treatments. The marked decrease in hydrogen uptake with increasing reduction temperatures appears to be related to decoration of Pt crystallites with reduced WO_x, as also proposed to explain similar effects in TiO_2 supported metal particles.

Table 5
Chemisorption of H_2, O_2, and CO on Pt/WO_x–ZrO_2 (0.3% wt. Pt, 10% wt. W)

	Irreversible chemisorption uptake [a] (H, O, or CO/Pt atom)		
Reduction temperature (K)	H_2	O_2	CO
473	0.63	1.25	0.30
623	0.092	2.04	0.050

[a] Room temperature adsorption: irreversibly chemisorbed species are defined as those that cannot be removed by evacuation at room temperature.

High isomerization rates appear to require the presence of WO_x domains of intermediate size, which form after oxidation at approx. 1000 K by controlled sintering of octahedral WO_3 clusters. These distorted octahedral domains have been detected by X-ray absorption and UV-visible spectroscopies [68,71] and differ markedly in electronic structure, reduction behavior and isomerization rate and selectivity from previously reported isolated tungstate groups supported on Al_2O_3. Temperature-programmed reduction measurements show that small WO_x clusters on ZrO_2 and large crystals of bulk WO_3 reduce at higher temperatures than those of intermediate size, which lead to highest isomerization rates [68]. The unique acid properties of WO_x domains of intermediate size appear to be related to their ability to form W^{6-n}–O_x–(n-H^+) centers under reducing reaction conditions at low temperatures. These centers are formed via interactions between Pt and W^{6+} sites mediated by the migration of hydrogen adatoms; these hydrogen adatoms also play a critical role in isomerization elementary steps, which benefit from bifunctional pathways made available from the concurrent presence of H_2 dissociation sites and Bronsted acid sites during hydroisomerization reactions (Schemes 10 and 11). These polyoxoanion clusters [$(WO_3)_x$] can stabilize carbocationic species by delocalizing the corresponding negative charge among several oxygen atoms, as previously proposed for heteropolyoxoanions with Keggin structures [72].

7.3. *Ethanol condensation reactions on Cu-Mg_5CeO_x catalysts*

Recent studies [73–75] show that aldol condensation reactions of ethanol on ZnO [73] and modified MgO [74,75] are strongly influenced by the presence of Cu sites. Cu sites appear to act as more than ethanol dehydrogenation sites and also influence the rate and selectivity of acetaldehyde condensation reactions. Metal sites also increase the rate of acid-catalyzed condensation reactions of acetone on H-ZSM5 [76].

Basic oxides catalyze the formation of higher oxygenates from aldehydes and alcohol reactants via aldol condensation chain growth pathways [25]. Mg_5CeO_x

Table 6
Effects of Cu- and K-loading on ethanol consumption and product formation on Mg_5CeO_x. (573 K, 4 kPa ethanol, balance He; initial rates in gradientless batch reactor.)

wt.% Cu	wt.% K	Ethanol Dehydrogenation		Rates of formation: Acetone		Butyraldehyde	
		Areal rate	Turnover rate	Areal rate	Turnover rate	Areal rate	Turnover rate
		r_1 [a]	r_1 [b]	r_2 [c]	r_1 [d]	r_3 [c]	r_3 [d]
0	0	4.0×10^{-9}	—	6.2×10^{-11}	6.5×10^{-5}	— [e]	— [e]
7	0.1	3.6×10^{-7}	0.24	3.0×10^{-9}	2.2×10^{-3}	4.5×10^{-10}	3.4×10^{-4}
7	1.0	2.4×10^{-7}	0.23	4.3×10^{-9}	1.8×10^{-3}	7.6×10^{-10}	3.2×10^{-4}
49	1.2	9.4×10^{-7}	0.24	4.4×10^{-8}	1.0×10^{-2}	1.2×10^{-9}	2.8×10^{-4}

[a] Rate of ethanol consumption, expressed in mol/m^2 s.
[b] Turnover rates per Cu surface atom, expressed in s^{-1}.
[c] Rates of product formation, expressed in mol/m^2 $MgCeO_x$ s.
[d] Turnover rates per basic site (from $^{13}CO_2/^{12}CO_2$ switch) in mol/mol CO_2 s.
[e] Not detected.

oxides promoted with Cu and K catalyze the synthesis of isobutanol from CO and H_2 via bifunctional pathways requiring methanol synthesis and aldol condensation sites [74,75,77]. The Ce component increases the density and strength of basic sites in MgO and the rate of base-catalyzed chain growth reactions [74,75]. Potassium titrates Bronsted acid sites that lead to undesired etherification and hydrocarbon formation reactions.

Reactions of ethanol on Cu–Mg_5CeO_x at 573 K lead to the formation of acetaldehyde, *n*-butyraldehyde and acetone as predominant products. Acetaldehyde concentrations increase rapidly to equilibrium levels that become independent of Cu content in $Cu_yMg_5CeO_x$ catalysts. The non-zero initial slope in the time evolution of acetone and *n*-butyraldehyde products (Fig. 4) would be unexpected if these products formed via sequential reactions of acetaldehyde gas phase intermediates. It appears that ethanol undergoes condensation reactions directly, without requiring its intermediate conversion to gas phase acetaldehyde. This suggests, in turn, that the ethanol dehydrogena-

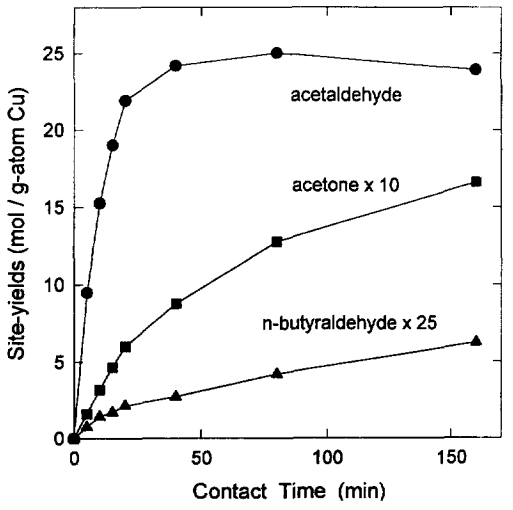

Fig. 4. Site yields as a function of contact time on (1.0 wt% K) $Cu_{0.5}Mg_5CeO_x$ in reactions of ethanol (573 K, 101.3 kPa total pressure, 4.0 kPa ethanol pressure, balance He).

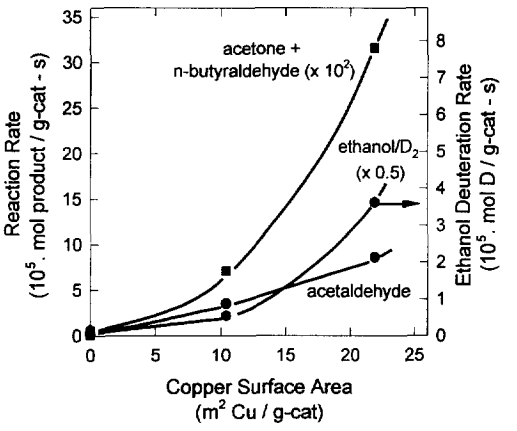

Fig. 5. Initial rates of ethanol dehydration and condensation reactions and of incorporation of deuterium into ethanol (in D_2–C_2H_5OH mixtures) as a function of Cu surface area on $Cu_yMg_5CeO_x$ catalysts (573 K, 101.3 kPa total pressure, 3.7 kPa ethanol (27 kPa D_2), balance He).

tion and condensation steps must occur on sites located within molecular distances, in view of the unlikely surface diffusion of ethoxide and related adsorbed species.

The initial rate of ethanol dehydrogenation increases linearly with the Cu surface area measured by N_2O decomposition methods, leading to turnover rates that are not affected by Cu crystallite size or by the presence of alkali (Table 6, Fig. 5). At similar steady-state acetaldehyde concentrations, chain growth rates to form acetone and n-butyraldehyde differ markedly on Mg_5CeO_x, (1.0% wt. K) $Cu_{0.5}Mg_5CeO_x$ and (1.0% wt. K) $Cu_{7.5}Mg_5CeO_x$ catalysts (Table 6, Fig. 5), even though basic site densities measured by CO_2 titration methods are very similar. This marked effect of Cu on chain growth rates shows that Cu metal sites participate in rate-determining steps required for condensation reactions.

Isotopic tracer studies using $^{12}C_2H_5OH$–$^{13}C_2H_4O$ reactant mixtures confirm that condensation reactions can proceed via direct reactions of ethanol, without the intermediate formation of gas phase acetaldehyde molecules [78]. These results suggest that 'dehydrogenation' and condensation reactions occur after binding of ethanol to the same type of active site, such as an acid–base site pair on MgO. These reactions, however, are influenced by the presence of Cu metal crystallites, which are unlikely to exist in atomic contact with a large fraction of MgO surface sites. Basic sites, however, may interact with Cu sites via migration of hydrogen atoms formed in C–H and O–H bond activation steps to Cu sites. These steps would lead to the reformation of hydrogen abstraction sites on MgO and to the elimination of the hydrogen reaction products as H_2 by recombinative desorption on Cu crystallites. If hydrogen removal is rate-determining in ethanol dehydrogenation and condensation reactions, Cu may provide the needed 'porthole' for its removal from MgO surfaces.

Acetaldehyde and ethanol condensation reactions occur on acid–base site pairs present in basic oxides. Infrared [79] and temperature-programmed surface reactions studies [74,75] suggest that the initial step in the activation of ethanol is the cleavage of OH bonds in ethanol to form adsorbed ethoxide species (on Mg^{+2}) and hydrogen atoms (on basic oxygens). Hydrogen species are removed by migration to Cu sites, reaction with another H species and desorption as H_2:

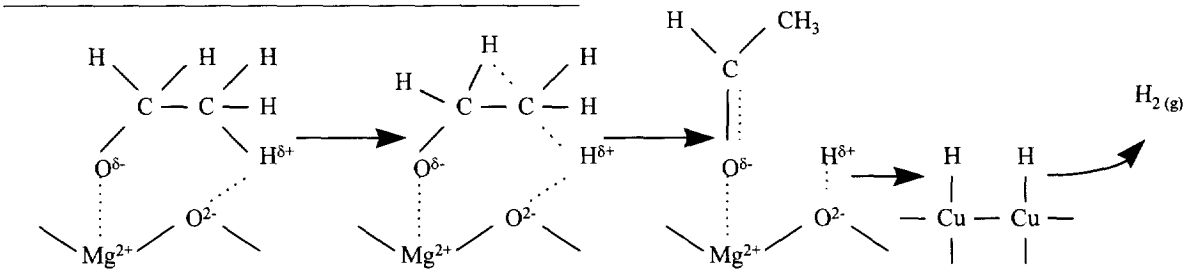

Ethoxide species, however, do not undergo condensation reactions and tend to re-form ethanol, unless hydrogen adatoms are removed by recombinative desorption processes. Several hydrogen abstraction steps are required to convert ethoxide to enolate-type species that can undergo aldol-type condensation reactions. These hydrogen abstraction steps will require the removal of previously formed H adatoms from basic oxygens in MgO acid–base pairs:

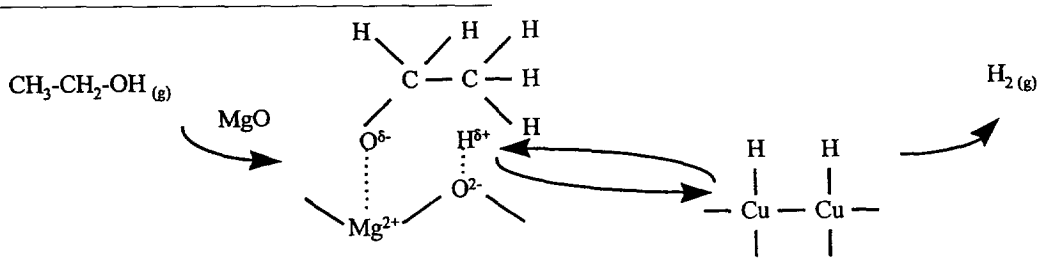

The migration to Cu sites provides a recombinative desorption pathway that is significantly less efficient on pure MgO or Mg_5CeO_x than on Cu-containing surfaces. C–H bond activation steps on acid–basic site pairs become kinetically coupled with hydrogen desorption steps catalyzed by Cu in order to increase the rate of formation of *n*-butyraldehyde and acetone during ethanol and acetaldehyde condensation reactions. Hydrogen migration on Mg_5CeO_x surfaces and recombinative desorption on Cu sites increase the rate of aldol condensation by removing a surface bottleneck that tends to reverse the step leading to the formation of unsaturated aldol-type species required for chain growth. This mechanistic proposal is consistent with the effect of Cu surface area on the rate of deuterium incorporation into the 'unreacted' ethanol in C_2H_5OH–D_2 reactant mixtures (Fig. 5).

The surface diffusion of hydrogen adatoms from basic oxygens to Cu sites and their recombination on Cu sites (and more slowly also on MgO) to form H_2 allows basic oxygens to be rapidly re-used as hydrogen abstraction sites. Adsorbed acetaldehyde species can desorb as acetaldehyde, or react with other surface species to form aldol condensation products. Once again, H species migrate from basic to Cu sites and recombine on Cu sites to form H_2:

Surface aldol species then undergo reactions via pathways well established in homogeneous base catalysis. In these reactions, the presence of copper sites enhances hydrogen transfer and provides H species for the hydrogenation of the unsaturated species, a step required for the desorption of condensation products.

These bifunctional condensation pathways are qualitatively similar in kinetic structure to those discussed earlier for C–H activation reactions of alkanes on cation-modified zeolites. They are consistent with the direct formation of aldol condensation products from the ethanol component in ^{12}C-ethanol/^{13}C-acetaldehyde mixtures and with the increased rate of isotopic exchange in C_2H_5OH/D_2 mixtures as the density of Cu surface atoms increases on the surface of Cu-Mg_5CeO_x catalysts.

8. Conclusions

Catalytic reactions of alkanes and alkanols frequently require multiple surface functions and concerted or sequential interactions with acid, base and H_2 dissociation sites. The activation of O–H and C–H bonds in these reactant molecules benefits from concerted interactions with acid–base site pairs. Solid

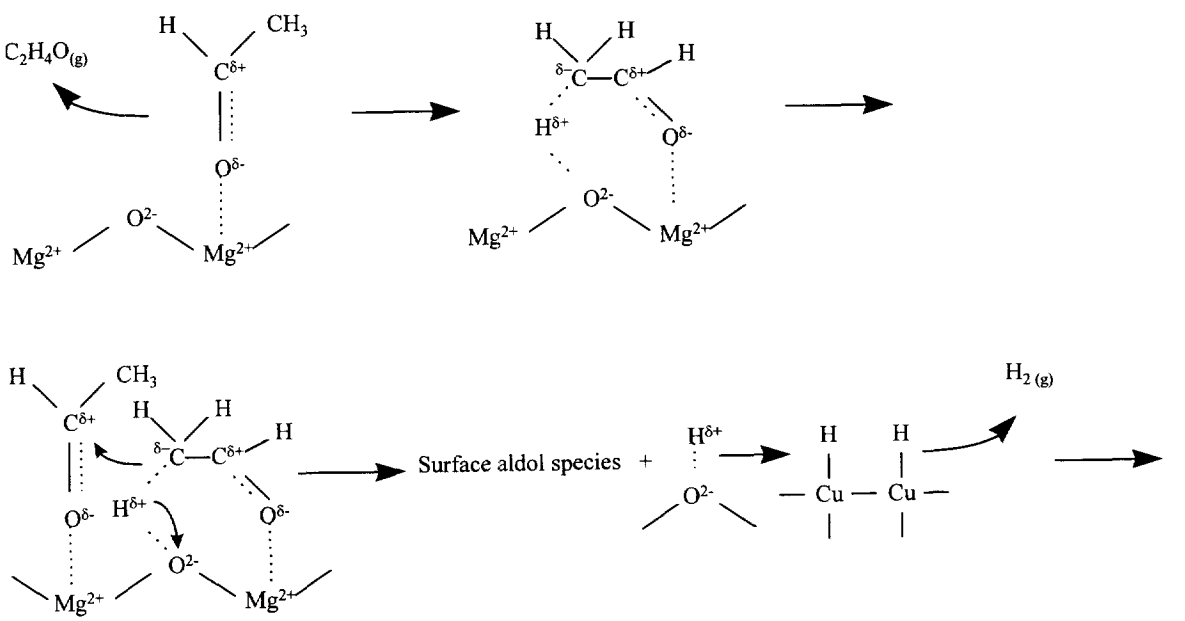

surfaces with weak acid–base site pairs catalyze hydrogenation and dehydration reactions with high selectivity, because of their ability to form and discard reaction intermediates during a catalytic turnover. The required site pairs may consist of conjugate acid–base pairs in single element oxides or may be introduced by a second component in binary oxides or supported metal oxide clusters.

Concerted interactions with several surface functions require that these functions exist within molecular distances. Non-concerted bifunctional pathways avoid this requirement and occur even when the required sites are located farther apart. Then, sites interact via the formation and migration of gas phase and surface species. Alkenes migrate between metal and Bronsted acid sites in catalytic isomerization and reforming reactions. The diffusion of hydrogen adatoms on surfaces provides a more effective interaction pathway than gas phase diffusion of alkenes for coupling acid-base site pairs and 'dehydrogenation' sites in alkane dehydrogenation and isomerization reactions and in condensation reactions of alcohols.

Acknowledgements

The authors would like to acknowledge financial support for this work from the National Science Foundation (CTS-9510575) and the Division of Fossil Energy of the U.S. Department of Energy (Contract DE-AC22-94PC94066). We would also like to thank Dr. Mingting Xu, Dr. Anne-Mette Hilmen and Ms. Brandy L. Stephens for helpful insights and technical discussions.

References

[1] C.G. Swain and J.E. Brown, J. Am. Chem. Soc., 74 (1952) 2534, 2538.
[2] R.P. Bell, The Proton in Chemistry. Cornell University Press, Ithaca, NY, 1959.
[3] K. Tanabe, Appl. Catal. 113 (1994) 147.
[4] K. Tanabe, in: K. Tanabe et al. (Eds.), Acid–Base Catalysis, Kodansha, Tokyo, 1989, p. 513.
[5] R. Breslow, J. Mol. Catal. 91 (1994) 161.
[6] T. Motomura, K. Inoue, K. Kobayashi and Y. Aoyama, Tetrahedron Lett. 32 (1991) 4757.
[7] J. Halpern, Adv. Catal. Rel. Subj. 11 (1959) 301.
[8] K.I. Zamaraev, V.M. Nekipelov and E.P. Talsi, Catal. Lett. 5 (1990) 127.
[9] G.A. Mills, H. Heinemann, T.A. Milliken and A.G. Oblad, Ind. Eng. Chem. 45 (1953) 134.
[10] P.B. Weisz and E.W. Swegler, Science 126 (1957) 31.
[11] F.G. Ciapetta, R.M. Dobres and R.W. Baker, in: P.H. Emmett (Ed.), Catalysis, Vol. 6, Reinhold, New York, NY, 1958, p. 510.
[12] K. Fujimoto and S. Toyoshi, Stud. Surface Sci. Catal. 7 (1980) 235; K. Fujimoto, in: T. Inui, et al. (Eds.), New Aspects of Spillover Effect in Catalysis, Elsevier, Amsterdam, 1993, p. 9.
[13] H. Knozinger, G. Buhl and K. Kochloeff, J. Catal. 24 (1972) 57.
[14] Y. Nakano, T. Yamaguchi and K. Tanabe, J. Catal. 80 (1983) 307.
[15] T. Yamaguchi, Y. Nakano and K. Tanabe, Chem. Lett., (1976) 677.
[16] B.Q. Xu, T. Yamaguchi and K. Tanabe, Chem. Lett., (1988) 281; Appl. Catal., 75 (1991) 75.
[17] K. Tanabe, Trends Anal. Chem. 13 (1994) 164.
[18] K. Tanabe and T. Yamaguchi, Catal. Today 20 (1994) 185.
[19] M. Boudart, A. Delbouille, E.G. Derouane, V. Indovina and A.B. Walters, J. Am. Chem. Soc. 94 (1972) 6622.
[20] R.L. Burwell, A.B. Littlewood, M. Cardew, G. Pass and C.T. Stoddart, J. Am. Chem. Soc. 82 (1960) 6272.
[21] T. Yamaguchi, H. Sasaki and K. Tanabe, Chem. Lett., (1973) 1017.
[22] A.J. Lundeen and R. Van Hoozer, J. Am. Chem. Soc. 85 (1963) 2180.
[23] M. Ueshima, Y. Shimasaki, K. Ariyoshi, H. Yano and H. Tsuneki, Stud. Surf. Sci. Catal. 75 (1993) 2447.
[24] T. Yokoyama, T. Setoyama, N. Fujita, M. Nakajima and T. Maki, Appl. Catal. 88 (1992) 149.
[25] H. Pines, The Chemistry of Catalytic Hydrocarbon Conversions, Academic Press, New York, NY, 1981.
[26] K. Tanabe and K. Saito, J. Catal. 35 (1974) 247.
[27] H. Kurokawa, W. Ueda, Y. Morikawa, Y. Moro-oka and T. Ikawa, in: K. Tanabe et al. (Eds.), Acid-Base Catalysis, Kodansha, Tokyo, 1989, p. 93.
[28] W. Ueda, T. Kuwabara, T. Ohshida and Y. Morikawa, J. Chem. Soc. Chem. Commun., (1990) 1558.
[29] W. Ueda, T. Ohshida, T. Kuwabara and Y. Morikawa, Catal. Lett. 12 (1992) 97.
[30] J.J. Spivey, M.R. Gogate and J.R. Zoeller, Am. Chem. Soc., Div. Petr. Chem. Prepr., 233 (1996).
[31] M.F. Hoq and K.J. Klabunde, in: K. Tanabe et al., (Eds.), Acid-Base Catalysis, Kodansha, Tokyo, 1989, p. 305.
[32] (a) A.L. Dent and R.J. Kokes, J. Phys. Chem., 73 (1969) 3372; (b) S. Coluccia, F. Boccuzzi, G. Ghiotti, and C. Morterra, J. Chem. Soc. Faraday Trans., 78 (1992) 2111.
[33] G.J. Kramer, R.A. van Santen, C.A. Emels and A.K. Nowak, Nature 363 (1993) 529.
[34] E.M. Evleth, E. Kassab and L.R. Sierra, J. Phys. Chem. 98 (1994) 1421.
[35] R.V. Dimitriev, K.H. Steinberg, A.N. Detjuk, F. Hofmann, H. Bremer and K.M. Minachev, J. Catal., 65 (1980) 105; L. Xu,

Z. Zhang, B. Marshik and W.M.H. Sachtler, Catal. Lett, 10 (1991) 121; S. Yu, J.A., Biscardi and E. Iglesia, unpublished results on H-ZSM5 and Zn/H-ZSM5.
[36] V.N. Kazansky and I. Senchenya, J. Mol. Catal. 74 (1992) 257; V.N. Kazansky, V.Y. Borovkov, and L.M. Kustov, Proc. 8th Int. Cong. Catal., Berlin, 3 (1984) 3.
[37] G.B. McVicker, G.M. Kramer and J.J. Ziemiak, J. Catal. 83 (1983) 286.
[38] H. Lauron-Pernot, F. Luch and J.M. Popa, Appl. Catal. 78 (1991) 213.
[39] M. Xu, Z. Hu, M.J.L. Gines, S.C. Reyes and E. Iglesia, J. Catal., submitted for publication.
[40] S. Bordiga, E. Garrone, C. Lambert and A. Zecchina, J. Chem. Soc. Faraday Trans. 90 (1994) 3367.
[41] F. Wakabayashi, J. Kondo, A. Wada and K. Domen, J. Phys. Chem. 97 (1993) 10761.
[42] H. Knozinger, in: K. Tanabe, H. Hattori, T. Yamaguchi and T. Tanaka (Eds.), Acid-Base Catalysis, Kodansha, Tokyo, 1989, p. 147; I. Mirsojen, S. Ernst, J. Weitkamp and H. Knozinger, Catal. Lett., 24 (1994) 235; F. Lange, K. Hadjiivanov, H. Schmelz and H. Knozinger, Catal. Lett., 16 (1992) 97.
[43] K. Tamaru, Dynamic Heterogeneous Catalysis, Academic Press, 1978; J. Happel, Isotopic Assessment of Heterogeneous Catalysis, Academic Press, New York, NY, 1986; S. Shannon and J.G. Goodwin, Chem. Rev., 95 (1995) 677.
[44] C. Grunding, G. Eder-Mirth and J.A. Lercher, J. Catal., 160 (1996) 299; G. Mirth, J. Ceijka and J.A. Lercher, J. Catal., 139 (1993) 24; J.A. Lercher, C. Grunding and G. Eder-Mirth, Catal. Today, 27 (1996) 353.
[45] E. Iglesia and J.E. Baumgartner, Catal. Lett., 21 (1993) 55; G.D. Meitzner, E. Iglesia, J.E. Baumgartner and E.S. Huang, J. Catal., 140 (1993) 209.
[46] F.H. Ribeiro, R.A. Dalla-Betta, M. Boudart and E. Iglesia, J. Catal., 130 (1991) 86; J. Catal., 130 (1991) 498.
[47] E. Iglesia, J.E. Baumgartner, F.H. Ribeiro and M. Boudart, J. Catal., 131 (1991) 523; Catal. Today, 15 (1992) 307.
[48] C. Pham-Huu, M.J. Ledoux and J. Guille, J. Catal. 143 (1993) 249.
[49] V. Keller, P. Wehrer, F. Garin, R. Ducros and G. Maire, J. Catal. 153 (1995) 9.
[50] M. Boudart, J.S. Lee, K. Imura and S. Yoshida, J. Catal. 103 (1987) 30.
[51] M. Boudart, J. Phys. Chem., 87 (1983) 2786; Ind. Eng. Chem. Fundam., 25 (1986) 70.
[52] H.S. Taylor, Annu. Rev. Phys. Chem. 12 (1961) 127.
[53] J. Kuriacose, Ind. J. Chem. 5 (1967) 646.
[54] E. Iglesia, J.E. Baumgartner and G.D. Meitzner, Stud. Surf. Sci. Catal. 75 (1993) 2353.
[55] J.A. Biscardi and E. Iglesia, Catal. Today 31 (1996) 207.
[56] T. Mole, J.R. Anderson and G. Creer, Appl. Catal. 17 (1985) 141.
[57] J. Yao, R. le van Mao and L. Dufresne, Appl. Catal. 65 (1990) 175.
[58] S. Khoobiar, J. Phys. Chem. 68 (1964) 411.
[59] M. Boudart, A.W. Aldag and M.A. Vannice, J. Catal. 18 (1970) 46.
[60] G.C. Bond, in: G.M. Pajonk et al. (Eds.), Spillover of Adsorbed Species, Elsevier, Amsterdam, 1983, p. 1.
[61] W.C. Conner Jr., in: Z. Paal and P.G. Menon (Eds.), Marcel Dekker, New York, NY, 1988, p. 311.
[62] W.C. Conner Jr., P.G. Menon and S.J. Teichner, Adv. Catal. 34 (1986) 1.
[63] B. Delmon and G.F. Froment, Catal. Rev.-Sci. Eng. 38 (1986) 69.
[64] M.I. Temkin and V. Pyzhev, Acta Physicochim., 12 (1940) 327; M. Boudart, Ind. Eng. Chem. Fundam., 25 (1986) 70.
[65] V.C.F. Holm and G.C. Bailey, US Patent 3, 032, 599 (1962); M. Hino and K. Arata, J. Chem. Soc. Chem. Commun., (1980) 851.
[66] M. Hino and K. Arata, Chem. Commun., (1987) 1259.
[67] E. Iglesia, S.L. Soled and G.M. Kramer, J. Catal. 144 (1993) 238.
[68] E. Iglesia, D.G. Barton, S.L. Soled, S. Miseo, J.E. Baumgartner, W.E. Gates, G.A. Fuentes and G.D. Meitzner, Stud. Surf. Sci. Catal. 101 (1996) 533.
[69] T. Shishido and H. Hattori, Appl. Catal. 146 (1996) 157.
[70] H. Ebitani, J. Tsuji, H. Hattori and H. Kita, J. Catal., 135 (1992) 609; T. Shishido and H. Hattori, Appl. Catal., 146 (1996) 157.
[71] D.G. Barton, G.D. Meitzner, S.L. Soled and E. Iglesia, unpublished results.
[72] M. Misono, Catal. Rev. Sci. Eng. 29 (1987) 269.
[73] M.J. Chung, D.J. Moon, H.S. Kim and S.K. Ihm, J. Mol. Catal. 113 (1996) 507.
[74] M. Xu, M.J.L. Gines, B.L. Stephens and E. Iglesia, Proc. 13th Int. Coal Conf., 1996, p. 1328.
[75] M. Xu, M.J.L. Gines, B.L. Stephens and E. Iglesia, J. Catal., 170 (1997) in press.
[76] T.J. Huang and W.O. Haag, US Patent 4 339 606 (1982); W.F. Holderich, in: K. Tanabe et al. (Eds.), Acid-Base Catalysis, Kodansha, Tokyo, 1989, p. 1; L. Melo, G. Gianetto, P. Magnoux and M. Guisnet, Actas XV Iberoam. Catal. Symp., (1996) 1225.
[77] C.R. Apesteguia, S.L. Soled and S. Miseo, US Patent 5,387,570 (1995).
[78] M.J.L. Gines and E. Iglesia, J. Catal., submitted.
[79] V.A. Ivanov, J. Bachelier, F. Audry and J.C. Lavalley, J. Mol. Catal. 91 (1994) 45.